



The effects of reactor material and convective heat transfer coefficient on methane catalytic partial oxidation in a micro-channel

Jing-yu Ran, De-xiang Yang and Li Zhang

Key Laboratory of Low-Grade Energy Utilization Technology and Systems, Ministry of Education (Chongqing University), Chongqing, China

ABSTRACT

By using detailed reaction mechanism of CH_4 catalytic oxidation on rh surface, the catalytic partial oxidation of low concentration CH_4 was investigated numerically in a micro-channel focusing on the effects of reactor material and convective heat transfer coefficient on it. The results show that: the reactor with different reactor materials and h has the fixed effect on methane catalytic partial oxidation. First, methane conversion of the outlet is 92.31% on ceramic reactor; X_{CH_4} is 96.1%, 96.5% and 96.9% in several other reactors. The material of big thermal conductivity such as stainless steel, corundum, red copper produces bigger yield of CO and H_2 than ceramic reactor. At the same time, high thermal conductivity has a problem of carbon deposition on the wall. Then, when h is $0 \text{ w}\cdot\text{m}^{-2}\cdot\text{k}^{-1}$, the methane conversion efficiency reaches 99.9%, yield coefficient of H_2 reaches 95.85%, yield coefficient of CO reaches 86.7%. The smaller h is, the more syngas we get in this reactor. In order to get more syngas and have stable combustion, just adopt the material of high thermal conductivity and keep the reactor adiabatic.

Keywords: Reactor material; convective heat transfer coefficient; low concentration CH_4 ; catalytic partial oxidation; numerical investigation

INTRODUCTION

In recent years, with the development of micro fabrication technology and micro-electro-mechanical systems (MEMS) [1-2], more and more researchers are aware of micro burners as a promising type of portable energy device. Micro burners have many advantages, such as the simple structure, long working life, easy fuel replacement, and providing powers from a number of microwatts to hundreds of watts. They have been widely applied to the military, aerospace, chemical analysis, biomedical, environmental monitoring, digital electronic products and other fields. Due to the low concentration of methane hard to be on fire, many scholars put forward to join the hydrogen to promote fire. POM is a good way to produce H_2 , which has high efficiency. Because of the problem of Carbon deposition; we add a small amount of water vapor in the reactor [3-4] which coupled partial oxidation reaction. These measures are just adopted for good combustion.

Now, many scholars have focused on POM. Sun Zhiwei et al [5] study the action of gravity on it by numerical methods. Carbon deposit has increased along the direction of gravity wall and reduced in the opposite direction. Tornaiainen et al [6] suggested that CH_4 has dissociation of carbon and hydrogen on the catalyst surface first, and then CO_2 . Yan qiang et al [7] adopted the experiment to research the carbon deposit. Mallens [8] used TAP to study the POM, and they think the reaction of CO is quicker than CO_2 . Walter et al [9] thought that CH_4 generated C_x and CH_x firstly. Wang Haiyan [10] obtains the developing tendency of outcrop coal fire under the multi - ventilation powers and fire pressure. Ashok V and An. Palaniappan [11-12] research the kinetics and mechanism of oxidation and cyclization-oxidation. Early some researches have played an important role to understand the methane/oxygen catalytic partial oxidation, but still

have some questions, such as reactor material and convective heat transfer coefficient which have effect on the production of synthesis gas. This paper uses the numerical method to learn the low concentration of CH₄ of partial oxidation reaction on Rh catalyst, focusing on reactor material and h on the characteristic of catalytic partial oxidation reaction of CH₄. The reaction mechanism is analyzed with detail; it lays a theoretical foundation for the further study on the combustion system.

1 PHYSICAL AND MATHEMATICAL DESCRIPTION

1.1 Physical model

The configuration of the 3-D micro-tube adopted in this paper is shown in Fig.1. The internal radius of the tube r_0 is 0.5 mm, the thickness of the wall is 0.1 mm and the whole length of the tube L is 10 mm. Rh catalysts is assumed to be uniformly deposited on the smooth inner-wall with a density of $2.72 \times 10^{-8} \text{ kmol} \cdot \text{m}^{-2}$. The center of the tube entrance locates at the origin of coordinates, and the inlet velocity of the mixture gas is uniform at the entrance of the tube and positive with x-axis. Catalytic combustion occurs at the surface of catalyst, which the gas reaction rate is quite slow compared to gaseous combustion.

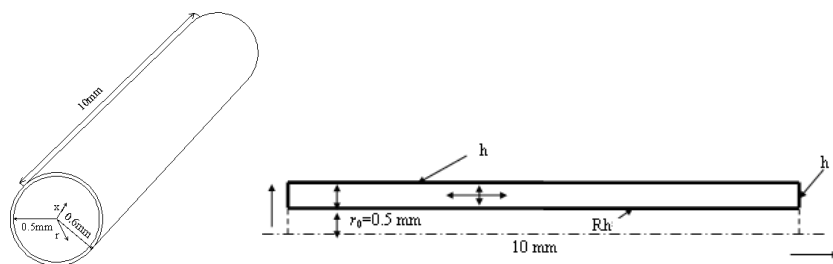


Fig.1 The schematic structure of circular tube

1.2 Numerical models

Though the micro-tube is millimeter-scale, its characteristic size is still much bigger than the average free distance of the reactant molecules. So it is reasonable to adopt continuum model in this paper. In addition, the body force term, dissipations and radiation of the gaseous species are neglected. The main governing equations are as follows.

Continuum equation,

$$\frac{\partial \rho}{\partial t} + \frac{\partial(\rho u)}{\partial x} + \frac{1}{r} \frac{\partial(r \rho v)}{\partial r} = 0. \quad (1)$$

Momentum equation,

$$\begin{aligned} \frac{\partial(\rho u)}{\partial t} + \frac{\partial(\rho u u)}{\partial x} + \frac{\partial(\rho v v)}{\partial r} = & -\frac{\partial P}{\partial x} + \frac{\partial}{\partial x} \left[\frac{4}{3} \mu \frac{\partial u}{\partial x} - \frac{2}{3} \mu \frac{1}{r} \frac{\partial(r v)}{\partial r} \right] \\ & + \frac{1}{r} \frac{\partial}{\partial r} \left[\mu r \left(\frac{\partial v}{\partial x} + \frac{\partial u}{\partial r} \right) \right] \end{aligned} \quad (2)$$

$$\begin{aligned} \frac{\partial(\rho v)}{\partial t} + \frac{\partial(\rho u v)}{\partial x} + \frac{\partial(\rho v v)}{\partial r} = & -\frac{\partial P}{\partial r} + \frac{\partial}{\partial x} \left[\mu \left(\frac{\partial v}{\partial x} + \frac{\partial u}{\partial r} \right) \right] \\ & + \frac{\partial}{\partial r} \left[\frac{4}{3} \mu \frac{\partial v}{\partial r} - \frac{2}{3} \mu \left(\frac{\partial u}{\partial r} + \frac{v}{r} \right) \right] + \frac{2\mu}{r} \left(\frac{\partial v}{\partial r} - \frac{v}{r} \right) \end{aligned} \quad (3)$$

Energy equation of the gas phase,

$$\begin{aligned} \frac{\partial(\rho h)}{\partial t} + \frac{\partial(\rho u h)}{\partial x} + \frac{\partial(\rho v h)}{\partial r} = & \frac{\partial}{\partial x} \left(\lambda_g \frac{\partial T}{\partial x} \right) + \frac{1}{r} \frac{\partial}{\partial r} \left(r \lambda_g \frac{\partial T}{\partial r} \right) + \frac{\partial}{\partial x} \left(\sum_{k=1}^{k_s} h_k \rho_k \frac{\partial Y_k}{\partial x} \right) \\ & + \frac{\partial}{\partial r} \left(\sum_{k=1}^{k_s} h_k \rho_k \frac{\partial Y_k}{\partial r} \right) - \sum_{k=1}^{k_s} h_k R_k M_k \end{aligned} \quad (4)$$

Species equation of the gas phase,

$$\frac{\partial(\rho Y_k)}{\partial t} + \frac{\partial(\rho u Y_k)}{\partial x} + \frac{\partial(\rho v Y_k)}{\partial r} = \frac{\partial}{\partial x}(\rho D_k \frac{\partial Y_k}{\partial x}) + \frac{1}{r} \frac{\partial}{\partial r}(r \rho D_k \frac{\partial Y_k}{\partial r}) + R_k M_k \quad (k = 1, 2, \dots, K_i) \quad (5)$$

Energy equation of the solid wall,

$$\frac{\partial(\rho h)}{\partial t} = \frac{\partial}{\partial x}(\lambda_s \frac{\partial T}{\partial x}) + \frac{1}{r} \frac{\partial}{\partial r}(r \lambda_s \frac{\partial T}{\partial r}) - \sum_{k=1}^{k_i+k_j} h_k S_k M_k \quad (6)$$

The ideal gas and caloric equation of state,

$$p = \rho R T \sum_{k=1}^{K_i} \frac{Y_k}{M_k} \quad (7)$$

D Diffusion coefficient ($\text{m}^2 \cdot \text{s}^{-1}$), p pressure, u, v Axial, radial velocities ($\text{m} \cdot \text{s}^{-1}$), h Total enthalpy of the gas phase ($\text{J} \cdot \text{K}^{-1} \cdot \text{g}$), K_i, K_j Total number of gaseous species and surface species, r Radial coordinate (m), x Axial coordinate (m), ρ Density ($\text{Kg} \cdot \text{m}^{-3}$), Thermal conductivity ($\text{W} \cdot \text{m}^{-1} \cdot \text{K}^{-1}$), Y Mass fraction, μ Viscosity ($\text{Pa} \cdot \text{s}$), Φ Methane/oxygen equivalence ratio.

1.3 Reaction mechanism

In a millimeter-scale catalytic combustor, homogeneous reaction is generally ignored, since it will be inhibited by the use of catalysts. So only a heterogeneous mechanism is included in the calculation of this paper. The detailed elementary heterogeneous mechanism of methane over Rh established by Deutschmann et al[13] is used in this paper.

2 CALCULATION METHOD AND MODEL VALIDATION

Laminar flow model and component transmission model is employed. The method for solving the problem is the SIMPLE algorithm. Import speed inlet boundary (the residence time of the gas mixture in the tube is much larger than the reaction time) and pressure outlet boundary are put to use. Inlet and outlet pressure are an atmospheric pressure. Inner wall uses the coupling wall. Wall has adopted different material in table one. These equations are used to have a detail on research. X_{CH_4} represents methane conversion; W_{H_2}, W_{CO} represents yield coefficient.

$$X_{CH_4} = \frac{n_{CH_4}^0 - n_{CH_4}}{n_{CH_4}^0} \times 100\% \quad (8)$$

$$W_{H_2} = \frac{n_{H_2}}{2 \times n_{CH_4}^0 + n_{H_2O}^0} \times 100\% \quad (9)$$

$$W_{CO} = \frac{n_{CO}}{n_{CH_4}^0} \times 100\% \quad (10)$$

Table 1 Property parameter values of different wall material

project	$\lambda[\text{w} \cdot \text{m}^{-1} \cdot \text{k}^{-1}]$	$\rho[\text{kg} \cdot \text{m}^{-3}]$	$C_p[\text{J} \cdot \text{kg}^{-1} \cdot \text{k}^{-1}]$
ceramic	2	2600	1464
stainless steel	16	7200	615
corundum	32	3940	37
red copper	387	8978	381

To verify the accuracy of the dynamic model, the physical model which was used in the literature [14] by Alessandro Donazzi is used in this paper, and this paper adopted the same working condition such as it in the literature[15]. As shown in Fig.2, the result between simulation and experiment has close agreement, so the mathematical model and reaction mechanism in this paper is correct.

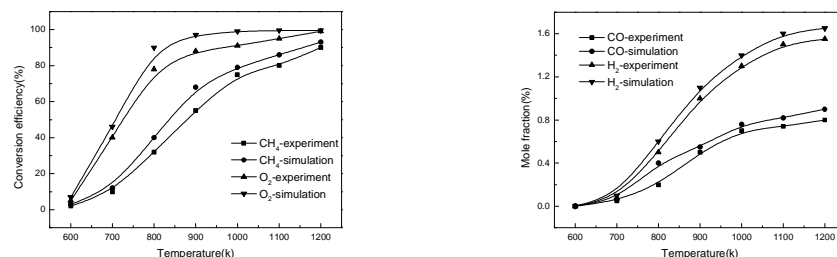


Fig.2 Computing validation (reaction airspeed $4 \times 10^6 \text{ Ni} \cdot \text{Kg}_{\text{cat}}^{-1} \cdot \text{h}^{-1}$, volume fraction of CH_4 1%, volume fraction of O_2 0.5%)

RESULTS AND DISCUSSION

3.1 The effects of reactor material on methane catalytic partial oxidation

The mixed gas is constituted by CH_4 , O_2 and N_2 . N_2 is an inert gas, and it does not participate in the reaction. Methane volume fraction is 5%; oxygen volume fraction is 2.5%, water vapor volume fraction of 1%. Inlet pressure is 1atm, and the convective heat transfer coefficient is $1 \text{ w} \cdot \text{m}^{-2} \cdot \text{k}^{-1}$. Preheating temperature of the mixed gas is 900k. As shown in Fig.3 and Fig.4, for different wall materials, oxygen consumption rate has little change, because oxygen is diffusion controlled, and the temperature gradient of different reactor has a little effect on it. X_{CH_4} (methane conversion) of the outlet is 92.31% in ceramic reactor, X_{CH_4} are respectively 96.1%, 96.5% and 96.9% in several other reactors. The smaller the coefficient of thermal conductivity is, the higher the temperature of the oxidation zone is, and the lower the temperature reforming zone is on the contrary. Methane conversion is high in the oxidized zone, but it is low in reforming area. Finally methane conversion of high thermal conductivity such as red copper is higher than others.

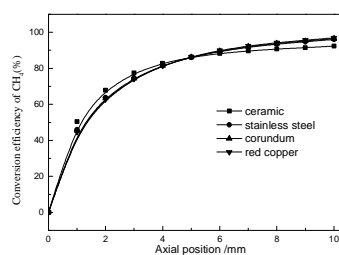


Fig.3 The axial concentration distribution of conversion efficiency of CH_4

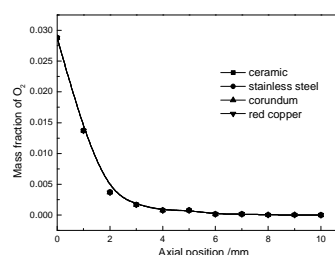


Fig.4 The axial concentration distribution of mass fraction of O_2

Fig.5 and Fig.6 shows that the reaction product yield is distributed in different material wall. Yield coefficient of H_2 (W_{H_2}) of the ceramic is higher in the reforming zone, but after 5mm from the inlet, it is lower than the other material. Finally W_{H_2} is 83.6% in ceramic reactor, and the others are respectively are 88.9%, 89.6% and 90.2%. As to the selectivity of the CO, W_{CO} is 84.4% in ceramic reactor, and others are respectively 87.4%, 87.7% and 87.9% else. Because the different material has different λ (Thermal conductivity). When the λ of the material is low, the heat loss is least than others.

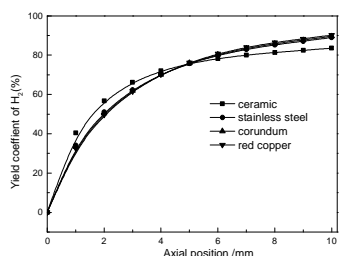


Fig. 5 The axial concentration distribution of yield coefficient of H_2

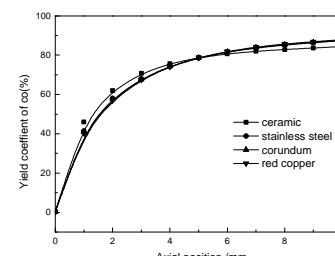


Fig. 6 The axial concentration distribution of yield coefficient of CO

From Fig.7, the axial change of the temperature in the ceramic reactor is large, but the heat loss is little. The heat loss of the ceramic reactor is 0.0265 w . The large λ is good for the heat transmitted to the upstream and downstream. At the same time, it can preheat the mixed gas. In order to get a high yield coefficient of CO and H_2 ; just use the material of high thermal conductivity, such as red copper. As shown in Fig.8, carbon deposition presents different with material. In

the ceramic reactor, the carbon deposition of surface coverage is 0.17, and the others are mainly 0.21. They have the difference of 0.04, and it just takes up 23.5% by the ceramic. Because the low heat loss of the ceramic reactor, the reactor has a higher temperature than the others. High temperature is beneficial to reforming reaction which decreases carbon deposition.

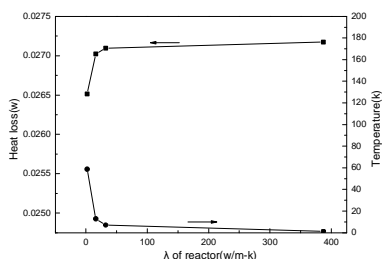


Fig.7 Heat loss and the max temperature difference of the wall

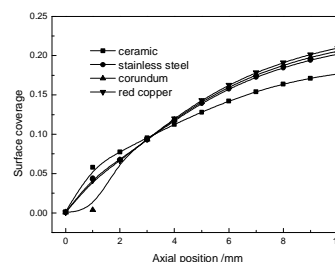


Fig.8 The axial concentration distribution of C(s) on the coupling wall surface

3.2 The effects of convective heat transfer coefficient out of the wall on methane catalytic partial oxidation

The mixed gas is constituted by CH_4 , O_2 and N_2 . N_2 is an inert gas, and it does not participate in the reaction. Methane volume fraction is 5%; oxygen volume fraction is 2.5%, water vapor volume fraction of 1%. Inlet pressure is 1atm, and the preheating temperature of the gas is 900k. As shown in Fig.9, the methane conversion efficiency appears different with surface convective heat transfer coefficient. When the wall is insulated, the methane conversion efficiency is maximal, and it reaches 99.9%. But in the convective heat transfer coefficient of $5\text{w}\cdot\text{m}^{-2}\cdot\text{k}^{-1}$, it only reaches 41.95%. Fig.10 shows that the consumption of oxygen keeps same with different h .

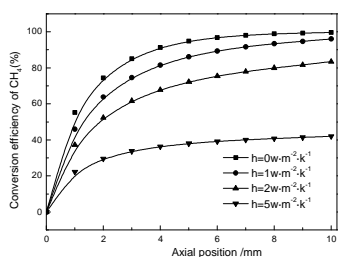


Fig.9 The axial concentration distribution of conversion efficiency of CH_4

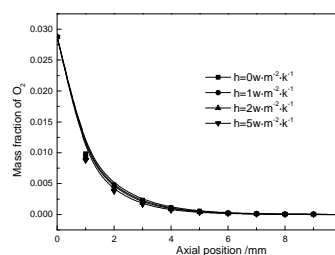


Fig.10 The axial concentration distribution of mass fraction of O_2

As shown in Fig.11 and Fig.12, yield coefficient of H_2 and CO perform variance with different h . When h respectively are 0、1、2 and $5\text{w}\cdot\text{m}^{-2}\cdot\text{k}^{-1}$, yield coefficient of H_2 reaches 95.85%、88.9%、71.6% and 17.7%. Methane happens strong reforming reaction and partial oxidation, when h is little which contributes to high temperature environment in the reactor. Yield coefficient of CO performs the same tendency as H_2 . When h respectively are 0、1、2 and $5\text{w}\cdot\text{m}^{-2}\cdot\text{k}^{-1}$, yield coefficient of CO reaches 86.7%、86.3%、75.7% and 29.5%.

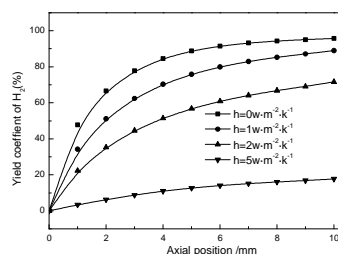


Fig. 11 The axial concentration distribution of yield coefficient of H_2

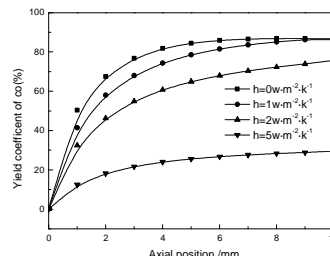


Fig. 12 The axial concentration distribution of yield coefficient of CO

From Fig.13, surface coverage changes a lot with h . When convective heat transfer coefficient changes from $0\text{w}\cdot\text{m}^{-2}\cdot\text{k}^{-1}$ to $5\text{w}\cdot\text{m}^{-2}\cdot\text{k}^{-1}$, surface coverage of carbon deposition reaches 0.27969548、0.20201814、0.13758537 and 0.048442189. The smaller h is, the smaller the heat transfer out of the wall is. When h is small, it just generates a high temperature environment which contributes to methane decomposition. As shown in Fig.14, the heat loss and the max temperature

difference of the wall changes with h . When h is respectively 0、1、2 and 5 $\text{w}\cdot\text{m}^{-2}\cdot\text{k}^{-1}$, heat loss is respectively 0、0.02702247 w 、0.05103969 w and 0.11107236 w . The max temperature difference increases with h which just makes reactor wall temperature uneven. To get more syngas and preheat the inlet gas well, keep the reactor adiabatic.

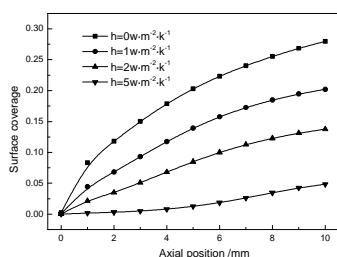


Fig.13 The axial concentration distribution of C(s) on the coupling wall surface

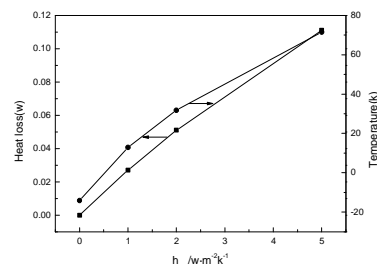


Fig.14 Heat loss and the max temperature difference of the wall

CONCLUSION

By using detailed reaction mechanism of CH_4 catalytic oxidation on Rh surface, the catalytic partial oxidation of low concentration CH_4 was investigated numerically in a micro-channel, focusing on the different material and convective heat transfer coefficient on it.

First, X_{CH_4} (methane conversion) of the outlet is 92.31% on ceramic reactor, X_{CH_4} is 96.1%, 96.5% and 96.9% in several other reactors. The bigger thermal conductivity of the material reactor is, the higher X_{CH_4} is. Then the big λ such as red copper has a high yield coefficient of H_2 and CO. The ceramic reactor has a small problem of carbon deposition, and the carbon deposition on the surface is not useful for the combustion. In order to get more syngas, we just adopt the material of high thermal conductivity. To different convective heat transfer coefficient, methane catalytic partial oxidation behaves different. When h is 0 $\text{w}\cdot\text{m}^{-2}\cdot\text{k}^{-1}$, the methane conversion efficiency reaches 99.9%, yield coefficient of H_2 reaches 95.85%, yield coefficient of CO reaches 86.7%. To get more syngas and preheat inlet gas well, keep the reactor adiabatic. When h is small, it has a relatively serious problem of carbon deposition which must be weakened in some methods. In conclusion, In order to get more syngas and have stable combustion, just adopt the material of high thermal conductivity and keep the reactor adiabatic.

Acknowledgment

This research was supported by National Natural Science Foundation of China (NSFC) (51276207, 50876118). We are grateful to Dr. Wu from University of Chongqing for his support of theoretical analysis.

REFERENCES

- [1] CC LOY; B Feng, *J. Power .Sources*, **2007**,165, 455-480.
- [2] H Epstein; SD Senturia, *Science*, **1997**, 276-1211.
- [3] JY Ran; JH Hu; L. Zhang; Q Tang, *Proceedings of the CSEE*, **2007**, 27, 43-48.
- [4] S Ding, C N Wu; Y H Cheng; Y Jin; Y Cheng, *Chem Eng Sci*, **2010**, 65, 1989-1999.
- [5] ZW Sun; L Zhang; YF Yan, *Chemical Industry and Engineering Progress*, **2012**, 31, 839-843.
- [6] PM Torniainen; X Chu; LD Schmidt, *J.Catal*, **1994**,146, 1-10.
- [7] QG Yan; TH Wu; JT Li, *Chinese Journal Of Applied Chemistry*, **1999**, 16, 20-23.
- [8] EP J Mallens; J H B Hoebink; GB Mstin, *J.Nat. Gas. Chem*, **2006**, 15, 21-27.
- [9] K Walter; OV Buyevskaya, *Catal. Lett*, **1994**, 29, 261-270.
- [10] HY Wang; ZHY Sun, *J.Chem.Pharm.Res.***2013**, 5(9):248-255
- [11] AK Borhade; DR Tope; DR Patil, *J.Chem.Pharm.Res.***2012**, 4(5):2501-2506
- [12] A Palaniappan; R Udhayakumar, *J.Chem.Pharm.Res.***2012**, 4(5):2385-2390
- [13] O Deutschmann; R. Schwiedernoch; I. Luba; C. DANIEL. *Studies in surface Science and Catalysis*, **2001**,136, 251-258.
- [14] A Aonazzi; A. Beretta; P. Forzatti. *J. Catal.* **2008**, 255, 241-258.
- [15] R. Horn; K. A. Williams; N. J. Degensterin, et al. *J. Catal.* **2006**, 242, 92-102.